

## RESEARCH ARTICLE

# Optical method supported by machine learning for dynamics of C-reactive protein concentrations changes detection in biological matrix samples

Patryk Sokołowski<sup>1</sup> | Kacper Cierpiak<sup>1</sup> | Małgorzata Szczerska<sup>1</sup>  |  
Maciej Wróbel<sup>1</sup>  | Aneta Łuczkiwicz<sup>2</sup> | Sylwia Fudala-Książek<sup>3</sup> |  
Paweł Wityk<sup>4,5</sup> 

<sup>1</sup>Department of Metrology and Optoelectronics, Faculty of Electronics, Telecommunications and Informatics, Gdańsk University of Technology, Gdańsk, Poland

<sup>2</sup>Department of Environmental Engineering Technology, Faculty of Civil and Environmental Engineering, Gdańsk University of Technology, Gdańsk, Poland

<sup>3</sup>Department of Sanitary Engineering, Faculty of Civil and Environmental Engineering, Gdańsk University of Technology, Gdańsk, Poland

<sup>4</sup>Department of Biopharmaceutics and Pharmacodynamics, Medical University of Gdańsk, Gdańsk, Poland

<sup>5</sup>Department of Molecular Biotechnology and Microbiology, Faculty of Chemistry, Gdańsk University of Technology, Gdańsk, Poland

## Correspondence

Paweł Wityk, Medical University of Gdańsk, 80-210 Gdańsk, Poland.

Email: [pawel.wityk@gumed.edu.pl](mailto:pawel.wityk@gumed.edu.pl)

## Funding information

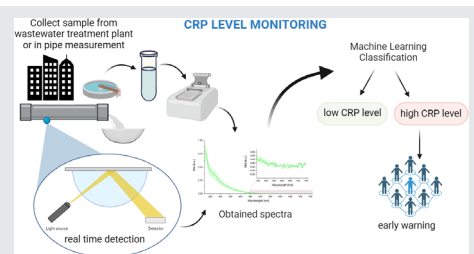
Politechnika Gdańska, Grant/Award Number: DS; Ministerstwo Edukacji i Nauki, Grant/Award Number: NdS/551425/2022/2022

## Abstract

In this article we present the novel spectroscopy method supported with machine learning for real-time detection of infectious agents in wastewater. In the case of infectious diseases, wastewater monitoring can be used to detect the presence of inflammation biomarkers, such as the proposed C-reactive protein, for monitoring inflammatory conditions and mass screening during epidemics for early detection in communities of concern, such as hospitals, schools, and so on. The proposed spectroscopy method supported with machine learning for real-time detection of infectious agents will eliminate the need for time-consuming processes, which contribute to reducing costs. The spectra in range 220–750 nm were used for the study. We achieve accuracy of our prediction model up to 68% with using only absorption spectrophotometer and machine learning. The use of such a set makes the method universal, due to the possibility of using many different detectors.

## KEYWORDS

biological matrix, biomarker, machine learning, optical method, spectroscopy, wastewater



## 1 | INTRODUCTION

C-reactive protein (CRP), an acute-phase reactant synthesized in the liver, has emerged as a pivotal biomarker in the assessment of inflammatory processes. Its quantification has

**Abbreviations:** BOD5, 5-day biochemical oxygen demand; COD, chemical oxygen demand; CRP, C-reactive protein; ML, machine learning; P.E., population equivalent; WWS, wastewater sample.

This is an open access article under the terms of the [Creative Commons Attribution](https://creativecommons.org/licenses/by/4.0/) License, which permits use, distribution and reproduction in any medium, provided the original work is properly cited.

© 2024 The Authors. *Journal of Biophotonics* published by Wiley-VCH GmbH.

been integral in clinical settings for diagnosing and monitoring various inflammatory conditions, with applications extending beyond individual patient care to broader public health contexts. This scientific introduction outlines the fundamental importance of CRP measurements, emphasizing the potential for mass screening during epidemics as a proactive strategy for early detection and intervention [1].

CRP serves as a sensitive and dynamic marker of systemic inflammation. Elevated CRP levels are indicative of a broad spectrum of pathological conditions, including infectious diseases, autoimmune disorders, and cardiovascular events. Its rapid and robust response to inflammatory stimuli positions CRP as a valuable tool for assessing the presence and severity of inflammatory processes [1, 2]. In the context of epidemic outbreaks, early detection of infections is paramount for effective public health management. CRP measurements offer a nonspecific yet highly sensitive indication of the body's response to infection, enabling timely identification of individuals with potential infectious diseases. The ability to monitor CRP levels at a population scale facilitates proactive health surveillance, aiding in the implementation of targeted interventions and resource allocation [3].

Epidemics, characterized by the rapid spread of infectious agents, demand innovative and scalable screening strategies for timely containment. Mass screening for CRP presents an opportunity to identify individuals with heightened inflammatory responses, serving as a proxy for early-stage infections. Integrating CRP measurements into large-scale screening programs can contribute to the identification of asymptomatic or presymptomatic carriers, thereby interrupting transmission chains and mitigating the impact of infectious diseases [4]. In the case of infectious diseases, wastewater monitoring can be used to detect the presence of the virus in communities of concern, such as hospitals, eldercare homes, kindergartens, schools, and so on. This information can help public health authorities make informed decisions regarding preventive and control measures, such as implementing targeted interventions and isolation protocols.

Implementing CRP-based mass screening during epidemics provides a data-driven approach for allocating resources efficiently. By stratifying individuals based on their CRP levels, public health authorities can prioritize testing, treatment, and quarantine measures for those at higher risk of infection or complications. This targeted approach optimizes the use of limited resources and enhances the overall effectiveness of public health interventions [5]. Recent technological advancements, including innovative optical methods supported by machine learning, have facilitated the development of rapid and scalable CRP measurement techniques. Integrating these technologies into mass screening programs enhances the feasibility of large-scale

testing, making it a practical and cost-effective strategy for epidemic preparedness and response [6]. In conclusion, the incorporation of CRP measurements into mass screening programs represents a paradigm shift in epidemic management, offering a proactive and data-driven approach to identify, isolate, and treat individuals at risk [7]. The significance of CRP as an inflammatory marker, coupled with technological advancements, underscores the potential of CRP-based mass screening as a crucial component of contemporary public health strategies during epidemics.

CRP is considered a biomarker of tissue damage, infection, or inflammation in the human body [8]. It is one of the most extensively studied markers commonly used to diagnose and monitor infections, especially in the emergency room or as a point-of-care test for differentiating bacterial from nonbacterial infections [9]. However, detecting CRP in wastewater might not be a common practice. Monitoring the presence level of CRP in wastewater might be used to track the spread of diseases or identify areas with increased morbidity. Based on monitoring system in wastewater treatment plants and in the sewage pipe inside the building the wastewater-based epidemiology can be applied [10, 11]. It is an emerging approach for community epidemiology surveillance. CRP level analysis may allow faster epidemic detection or assist in tracking the effectiveness of health interventions within a population. Thus, wastewater monitoring provides a complementary approach to traditional clinical diagnostic methods and has been recognized by the World Health Organization (WHO) as a useful tool to effectively combat epidemics. The development of new biosensors for online, real-time detection of infectious agents will eliminate the need for time-consuming processes, such as sample preparation, RNA extraction, or polymerase chain reaction (PCR). The proposed optical method is based on absorption measurement, allowing the determination of the changes in radiation intensity. The amount of absorbed radiation depends on the concentration, also CRP. The use of spectroscopic methods creates a very versatile method with easy change of source and detector. The advantage of this solution is the ability to install measuring device in wastewater system, but also possibility to use portable spectrophotometers in the field. Additionally, in this study, the measurement signals obtained from the biosensor were used to generate datasets utilized in machine learning models. This predictive capability can be instrumental in providing early warnings and identifying potential infection outbreaks, allowing for timely intervention and control measures to limit the spread of viral particles. This study also underlines the need for validation and rigorous testing to ensure their reliability and accuracy, which is crucial for the successful implementation of biosensors in disease surveillance and outbreak prediction.

## 2 | EXPERIMENTAL SECTION

In this study, wastewater sample (WWS) was used as the biological matrix. WWS contains a mix of organic and inorganic components, particles. Biological material in WWS was derived from bodily fluids and environment. Optical methods were used for the study. The absorbance measurements [12, 13] offer a monitoring of composition change present in the WWS. To detect changes of CRP concentration level in wastewater sample UV-Vis spectroscopy was used. The obtained absorbance measurements from WWS are compared with the support of machine learning. Figure 1 shows a diagram of the experiment.

### 2.1 | Material

WWS from sewage plant “Dębogórze” located in the Pomerania region (northern Poland) were collected. The treatment plant load is estimated at 440.000 P.E. For CRP study, samples collected for 3 months, during the period of August–October 2023, were used. During the mentioned period, a total of 14 WWS were taken from different days.

Investigated WWS are defined based on physical, chemical, and biological characteristics [14]. The parameters that the sewage plant monitors were determined by chemical oxygen demand (COD), 5-day biochemical oxygen demand (BOD5), suspended solids, alkalinity, temperature, pH, electrical conductivity, nitrogen, and phosphate. Table 1 presents the average value of parameter for WWS.

To investigate if the proposed optical method can detect changes in level of CRP, we prepared several solutions by adding CRP (90%–95% purity, Merck, Germany) to WWS at known concentration. From each WWS collected, another four samples were created with CRP concentrations ranging from  $10^{-4}$  to  $10^{-1}$   $\mu\text{g/mL}$ . Usually, CRP concentration in urine of healthy patients is 100  $\mu\text{g/mL}$  [15]. Taking dilution into account in WWS we can work with the lower range of CRP concentration to monitor the elevation of its level. Since the composition of WWS is constantly changing, there is a need to train an algorithm to distinguish whether an increase in chemical compounds will interfere with the detection of an increase in CRP levels. Thus, additional mixes of different WWS were created to ensure as much diversity as possible.

### 2.2 | Experimental methods

WWS before investigation was characterized by Raman spectroscopy. For the measurements, the WWS were dried. Raman spectra were recorded using an in-house made Raman spectroscopy system which consists of: spectrograph with about  $8\text{ cm}^{-1}$  resolution (HT Raman, EmVision llc, FL, USA), a TE-cooled CCD camera (iDus 420 BR-DD, Andor, UK) with 830 nm excitation wavelength laser with output power of 500 mW (Innovative Photonics Solutions, NJ, USA), and a fiber-optics contact probe with large working area of about  $0.5\text{ mm}^2$  spot size (EmVision llc, FL, USA). Raman spectra were acquired from samples of sewage which were dried in standard conditions for about 30 min on clean polished aluminum substrates, and measured with a probe at its focal point, near-contact. The detector was cooled to  $-60^\circ\text{C}$ , and the measurement time was set to 1 s with 20 averages, with the optical power at the probe output of about 50 mW as to not damage or burn the sample. The signal-to-noise ratio was on average equal 20, which means that the signal is of acceptable quality, although it can be further improved.

For further study, the absorption spectroscopy was used. Spectra were recorded for WWS and with different concentrations of CRP. To register signals, a NanoDrop

TABLE 1 Wastewater sample characteristics.

Parameters	Value	Unit
COD	1268.4	$\text{mgO}_2/\text{dm}^3$
BOD5	614.2	$\text{mgO}_2/\text{dm}^3$
Suspension solids	561.7	$\text{mg}/\text{dm}^3$
Alkalinity	9.8	$\text{mg}/\text{dm}^3$
Kjeldahl nitrogen	97.2	$\text{mg N}/\text{dm}^3$
Ammonium nitrogen	69.8	$\text{mg N}/\text{dm}^3$
Organic nitrogen	27.4	$\text{mg N}/\text{dm}^3$
Total nitrogen	97.2	$\text{mg N}/\text{dm}^3$
Orthophosphate	5.9	$\text{mg P}/\text{dm}^3$
Total phosphate	12.3	$\text{mg P}/\text{dm}^3$
Electrical conductivity	936	$\mu\text{s}/\text{cm}$
Temperature	16.4	$^\circ\text{C}$
pH	7.8	

Abbreviations: BOD5, 5-day biochemical oxygen demand; COD, chemical oxygen demand.

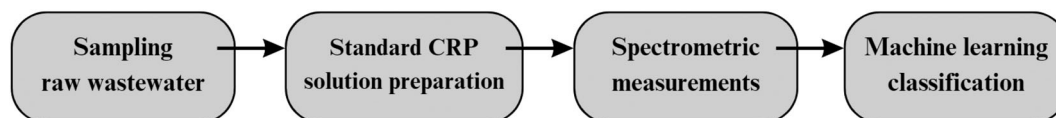


FIGURE 1 Experiment diagram with the four main steps of the method.

ND-1000 (Thermo Fisher Scientific, Inc., Waltham, MA, USA) spectrophotometer with a wavelength range of 220–750 nm, with accuracy of 1 nm was used. The device wavelength resolution is 3 nm and measured absorbance accuracy of 2%. A sample volume of 2  $\mu\text{L}$  is used for the measurement.

The UV–Vis spectrum changes with WWS composition, thus it can be used as an indicator to monitor dynamic changes in composition. The spectrum of WWS consists of high absorption at the beginning of the measurement range. However, the entire spectrum is used to monitor the dynamics of CRP concentration changes. Data at wavelengths above 450 nm, despite the low intensity of the signal can be significant. By using machine learning (ML) it is possible to search for correlations between spectrum and CRP changes.

### 2.3 | Classification

With the support of ML obtained spectra were put into classification. The aim was to divide the samples into two groups. The first group with samples having CRP concentrations below  $10^{-4}$   $\mu\text{g}/\text{mL}$  and the second group contained samples with CRP concentration above  $10^{-4}$   $\mu\text{g}/\text{mL}$ . This division allows to monitor CRP concentration in WWS.

Classification is a fundamental concept in machine learning that involves assigning data points to predefined categories or classes based on their characteristics. This process is analogous to sorting objects into different boxes based on their attributes. Classification algorithms learn from labeled data, which means that the data points in the training set are already associated with their respective categories. As the algorithm analyzes the training data, it identifies patterns and relationships between the data points and their corresponding classes. These patterns are then used to classify new, unlabeled data points by assigning them to the most likely class based on their characteristics [16–18].

The data preparation phase involved filtering the data and identifying signal peaks. Feature engineering and selection techniques were applied to extract relevant features for ML algorithms. With this process seven key features were identified and summarized in Table 2. To evaluate the significance of each feature, the importance permutation method was employed. This method assesses individual feature importance by measuring the change in model performance when a feature's values are randomly permuted. Critical features should significantly impact performance when permuted, while less important features should minimally affect performance [19, 20].

Three of the selected features F1, F6, and F7 need a more detailed explanation, as they are directly related to

TABLE 2 Summary of the features used in the model, along with their descriptions and their relative importance.

Features	Description	Feature importance
F1	Peaks prominence standard deviation	0.168
F2	Power density standard deviation value over the full measured range	0.157
F3	Median absolute deviation (MAD) of power density over the range between the first and last peak	0.151
F4	Power density variance value over the full measured range	0.150
F5	Geometric mean of the power density over the range between the first and last peak	0.133
F6	Peaks width standard deviation	0.121
F7	Peaks width variance	0.120

the peaks present in spectra and, more specifically, to the metrics that describe these peaks. Feature F1 uses a measure describing how much the peak stands out from its surroundings (Peaks Prominence), while features F6 and F7 are based on the width of the peaks (Peaks Width). A graphical interpretation of the basic metrics used to define peaks is shown in Figure 2.

Our research utilized a binary classification approach hence the division of the dataset into two classes: one representing samples with CRP concentrations below  $10^{-4}$   $\mu\text{g}/\text{mL}$  and the other including samples with CRP concentrations exceeding  $10^{-4}$   $\mu\text{g}/\text{mL}$ . This perfectly balanced dataset contains 540 samples in each group, amounting to a total of 1080 samples. However, excessive emphasis on training data can lead to overfitting, compromising the model's performance. To address this issue, we perform a training-validation split, allocating 723 samples to the training set and 357 samples to the validation set. This approach allowed us to effectively evaluate the model's performance as it prepares for its real-world application, enabling us to identify potential overfitting and make adjustments to ensure that the model generalizes well to new data. This process is crucial for developing robust and accurate ML models [21].

## 3 | RESULTS

### 3.1 | Spectrometric characterization

Raman spectrum presented in Figure 3 shows the data for a dried sample of WWS. The signal is not very strong



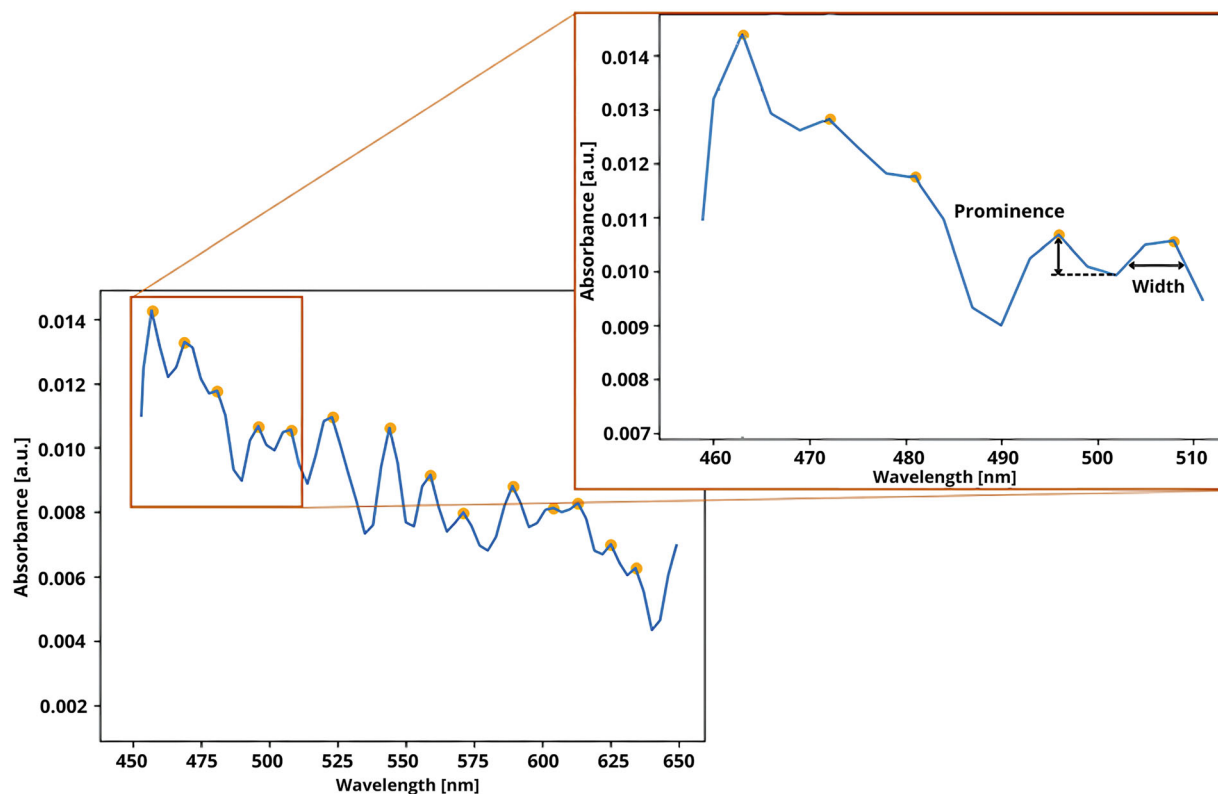


FIGURE 2 Graphical explanation of the prominence and width metrics used to describe the peaks.

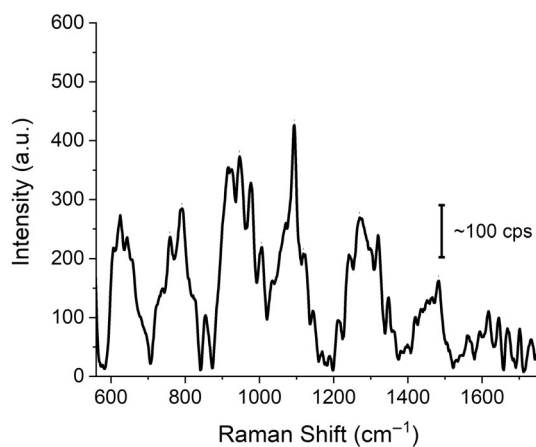


FIGURE 3 Raman spectra of dried wastewater sample.

with entirety of the spectrum signal encompassing about 500 counts per seconds (cps), with the bar in Figure 3 showing about 100 cps, yet after normalization, background removal and smoothing a viable spectrum is achieved. Specific identification of the origin of the peaks is difficult because the spectrum is a mixture of largely organic matter and inorganic sediments from WWS. The most prominent peaks with their possible assignments are at about  $1482\text{ cm}^{-1}$  C–H rocking,  $1319\text{ cm}^{-1}$  –OH,

$1269\text{ cm}^{-1}$  amide III,  $1094\text{ cm}^{-1}$  C–C stretch,  $787\text{ cm}^{-1}$  C–H bending,  $621\text{ cm}^{-1}$  ring deformation, and broadband in regions about  $1400\text{--}1480\text{ cm}^{-1}$  CH<sub>2</sub> and CH<sub>3</sub>,  $1200\text{--}1300\text{ cm}^{-1}$ , and  $900\text{--}1000\text{ cm}^{-1}$ .

The Raman spectra were shown to present additional information available by the means of molecular spectroscopy method, which not only shows its similarity to other spectra in the literature, but also proves lack of additional impurities and contamination of the sample which would cause gross errors in other methods which the article focuses on extensively. Also there are not many raw sewage Raman spectra provided in the literature, thus we find it valuable to present these results in the scope of our further research.

### 3.2 | Spectrometric measurements

The proposed CRP monitoring method in WWS is based on absorbance measurement. Thus, absorbance characterization was carried out. The UV–Vis spectroscopy in range  $220\text{--}750\text{ nm}$  was used for measurement as it was for the entire study. Figure 4 shows obtained absorbance characteristics of WWS. As reference value—blank—the ultrapure water was used. The blank value was subtracted from obtained WWS spectra. The bold line

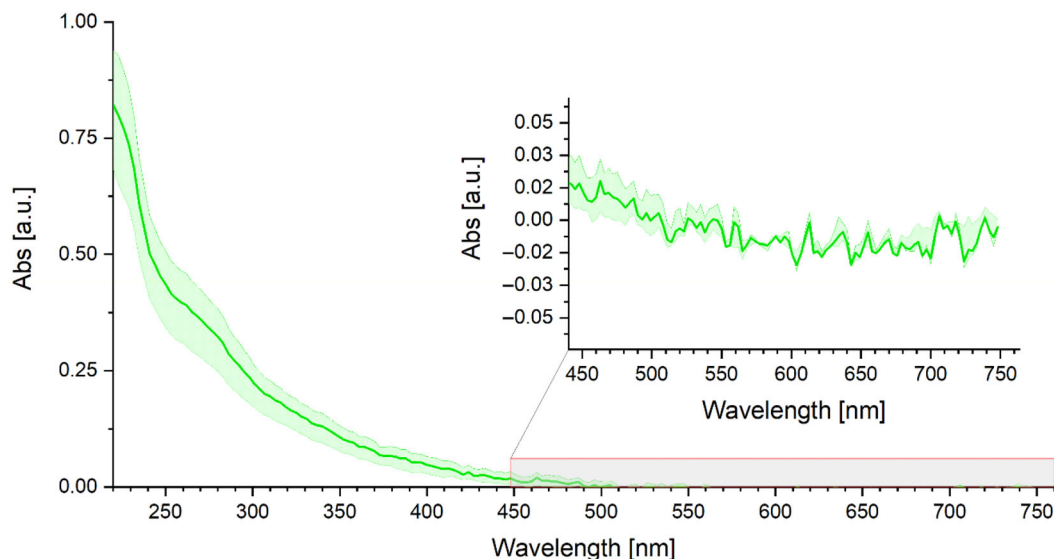


FIGURE 4 Absorbance characteristics of wastewater sample.

indicates the arithmetic mean value. The upper and lower values are reported as shaded areas.

The observed absorbance characteristics of WWS, as illustrated in Figure 4, highlight the dynamic nature of the UV–Vis spectrum in response to changes in WWS content. The high absorption at the beginning of the spectrum suggests the presence of substances with strong absorbance in the UV range (organic matter, e.g., proteins). However, it was observed that using the entire range of the spectroscope does not affect the obtained accuracy. By cutting out the UV range, the method will be quicker and more affordable (cheaper detectors). In the measured range, many compounds found in WWS affect the spectrum. This variability in absorbance serves as a promising indicator for monitoring changes in the composition of WWS. The successful detection of CRP in WWS validates the efficacy of the proposed optical method with the cutoff value of  $10^{-4}$   $\mu\text{g/mL}$ . The ML algorithm, trained on a diverse dataset that includes variations in WWS composition, demonstrates the adaptability of the system to the dynamic nature of environmental samples. This integrated approach holds great promise for real-time monitoring and early detection of elevated CRP concentrations in WWS during epidemic scenarios, contributing to proactive public health management. Further studies will explore the scalability and applicability of this method in diverse environmental settings.

### 3.3 | Machine learning analysis of wastewater sample spectra

Subsequently, we trained five models based on the ExtraTrees, RandomForest, XGBoost, DecisionTree, and

TABLE 3 Accuracy score of machine learning models.

Model	Accuracy
ExtraTrees	68.1%
RandomForest	66.7%
XGBoost	65.6%
DecisionTree	61.9%
KNeighbors	60.5%

TABLE 4 Summary of ExtraTrees Classifier algorithm performance using confusion matrix.

		Predicted class	
		Negative (CRP $\leq 10^{-4}$ $\mu\text{g/mL}$ )	Positive (CRP $> 10^{-4}$ $\mu\text{g/mL}$ )
Actual class	Negative	118	61
	Positive	53	125

KNeighbors algorithms. These five algorithms were chosen for their distinct strengths and weaknesses. This diversity enables a comprehensively nuanced assessment of different learning approaches and a deeper understanding of dataset characteristics. It is noteworthy that these algorithms are widely used and well established in the field of machine learning, especially for classification tasks. Their popularity provides a wealth of knowledge and resources available for implementing, fine-tuning, and evaluating models. The resulting prediction accuracy for each model is presented in Table 3. Interestingly, each of the selected algorithms exceeded the 60% accuracy, where the best result was achieved by the model based

TABLE 5 The characteristic of representative method for detection of C-reactive protein (CRP).

Name	Accuracy	Processing time	Limit of detection	Sample	DOI
Proposed solution	68.1%	Near-real time	0.1 µg/L	Wastewater	N/A
Fiber sensor	-	<10 min	5.65 µg/L	CRP standardized solution	[7]
Chemiluminescence in microfluid	-	30 min	15.5 µg/L	Clinical samples	[23]
Photonics crystal	-	5 min	12.24 ng/L	Human serum	[22]
Surface plasmon resonance	-	10 min	9 µg/L	Human serum	[28]
Enzyme-linked immunosorbent assay	-	Near-real time	1 µg/L	PBS and serum	[26]
Voltametric	-	-	0.5 µg/L	Human serum	[25]
Detection base on electrocardiograms	69.9%	-	5 mg/L	-	[24]

on the ExtraTrees algorithm achieving a score of over 68% accuracy.

To further evaluate the performance of the ExtraTrees model, a confusion matrix was prepared and is shown in Table 4. To simplify the table descriptions, it was assumed that samples containing a CRP concentration less than or equal to  $10^{-4}$  µg/mL would be labeled as negative, while samples containing a concentration greater than  $10^{-4}$  µg/mL would be labeled as positive. Out of 179 negative samples, the model correctly identified 118 as negative (True Negatives) and misclassified 61 as positive (False Positives). For the 178 positive samples, 125 were correctly classified as positive (True Positives) and 53 were misclassified as negative (False Negatives). These results indicate that the ExtraTrees model exhibits reasonable accuracy in classifying CRP levels into the two categories.

## 4 | DISCUSSION

Identifying the CRP level stands as a crucial part of diagnostics. Among others, the optical methods but not only are successfully applied. Table 5 shows the comparison of methods for detection of CRP. Of the presented methods, the solution using photonic crystal has the lowest detection concentration of 12.24 ng/L [22]. The method, which uses a fiber optic sensor, features detection from a concentration of 5.65 µg/L [7]. The advantage of this method is the small size of the sensor. The method using microfluids has reach detection 15.5 µg/L requires a very small sample volume [23]. The disadvantage of this method in particular applications may be the long processing time of 30 minutes. It was an interesting idea to measure CRP from analysis of electrocardiograms with machine learning obtained the accuracy of CRP level prediction of 69.9% [24]. A method with a very good level of detection 0.5 and 1 µg/L are voltametric [25] and most recent clinical method using the Enzyme-linked immunosorbent assay (ELISA) [26]. The assays usually require to use human plasma derived from

blood of patient and are based on antibody/CRP interaction. Some of the assays like ELISA can be used to determine the concentration of CRP in different biofluids like urine or wastewater, due to the nature of the diagnostic test [27]. The advantage of ELISA method is enabling measurements in almost real time. Nevertheless, the methods for CRP determination in clinical practice are more or less the same for past decades.

The table shows that a challenge of CRP detection system is to get the limit of detection as low as possible and to get the measurement time as short as possible. The main advantage of the proposed method is to use an optical system, that allows to monitoring dynamic of CRP level changes in near-real time. Additionally, the method enables detection in collected sample but also allows to install measurement system with minimal modification to existing sewer systems. This means that the device can monitor CRP in a way that does not require sampling by man. The proposed measurement range allows to use unexpensive optoelectronic elements, though the system can be installed in many nodes of the sewer network. This will enable dynamic of changes of increased morbidity in different parts of the city or building for early warning.

## 5 | CONCLUSION

Monitoring the CRP presence in WWS has the potential to track disease spread and identify regions with heightened morbidity. Analyzing CRP levels could expedite epidemic detection and aid in evaluating the efficacy of health interventions across populations. The proposed optical method with ML support can be widely used in places such as schools, hospitals, and office buildings. The development of new biosensors for online, real-time detection of infectious agents will eliminate the need for time-consuming processes, such as sample preparation, RNA extraction, or PCR and at the same time, it will

reduce monitoring costs. The advantage of the solution is processing time and versatility, the measurement equipment can also be used for other spectrophotometric measurements.

The chemical composition of WWS is constantly changing. These are significant changes as can be observed in the presented characteristics for WWS. This affects the work of ML algorithms. Despite of that we achieve accuracy of our prediction model up to 68% with using only simple spectrophotometer and machine learning. No additional markers or sensor modifications were used for the wastewater matrix.

Monitoring WWS over a longer period could help to better teach the algorithms to detect dynamics changes of CRP concentrations with higher accuracy. It could help the method to become more resistant to erroneous detection caused by an increase above the standard of another biological matter present in WWS.

## AUTHOR CONTRIBUTIONS

**Conceptualization:** Paweł Wityk and Małgorzata Szczerska. **Methodology:** Patryk Sokołowski and Małgorzata Szczerska. **Sample collection:** Aneta Łuczkiewicz and Sylwia Fudala-Książek. **Sample preparation:** Patryk Sokołowski and Paweł Wityk. **Investigation and writing—original draft preparation:** Patryk Sokołowski, Paweł Wityk, and Kacper Cierpiak. **Raman spectroscopy measurement:** Maciej Wróbel. **Spectroscopy measurement:** Patryk Sokołowski. **Measurement data processing and analysis:** Kacper Cierpiak. **Writing—review and editing:** Paweł Wityk and Małgorzata Szczerska. All authors have read and agreed to the published version of the manuscript.

## ACKNOWLEDGMENTS

The project is co-financed by DS programs of Faculty of Electronics, Telecommunications and Informatics of Gdańsk Tech, and by the Nds/551425/2022/2022 grant under the Ministry of Education and Science program is gratefully acknowledged. The authors would like to acknowledge Ying Hsueh Chen for helping during the spectroscopic measurements.

## CONFLICT OF INTEREST STATEMENT

The authors declare no conflicts of interest.

## DATA AVAILABILITY STATEMENT

The data that support the findings of this study are available from the corresponding author upon reasonable request.

## ORCID

Małgorzata Szczerska  <https://orcid.org/0000-0003-4628-6158>

Maciej Wróbel  <https://orcid.org/0000-0002-4521-0760>

Paweł Wityk  <https://orcid.org/0000-0001-8612-727X>

## REFERENCES

- [1] R. Ramamoorthy, V. Nallasamy, R. Reddy, N. Esther, Y. Maruthappan, *J. Pharm. Bioallied Sci.* **2012**, *4*, 422.
- [2] N. A. Martínez-González, E. Keizer, A. Plate, S. Coenen, F. Valeri, J. Y. J. Verbakel, T. Rosemann, S. Neuner-Jehle, O. Senn, *Antibiotics* **2020**, *9*, 1.
- [3] P. Barroso, D. Relimpio, J. A. Zearra, J. J. Cerón, P. Palencia, B. Cardoso, E. Ferreras, M. Escobar, G. Cáceres, J. R. López-Olvera, C. Gortázar, *One Health* **2023**, *16*, 100479.
- [4] R. Haneef, S. Kab, R. Hrzic, S. Fuentes, S. Fosse-Edorh, E. Cosson, A. Gallay, *Arch. Public Health* **2021**, *79*, 1.
- [5] J. Cooke, C. Llor, R. Hopstaken, M. Dryden, C. Butler, *BMJ Open Respir. Res.* **2020**, *7*, e000624.
- [6] J. Qin, M. Li, Y. Liang, *Inf. Fusion* **2022**, *80*, 121.
- [7] M. Szczerska, M. Kosowska, R. Viter, P. Wityk, *J. Biophotonics* **2023**, *16*, e202200213.
- [8] M. D. Sonawane, S. B. Nimse, *Anal. Methods* **2017**, *9*, 3400.
- [9] J. W. L. Cals, M. H. Ebell, *Br. J. General Pract.* **2018**, *68*, 112.
- [10] C. Oh, A. Zhou, K. O'Brien, Y. Jamal, H. Wennerdahl, A. R. Schmidt, J. L. Shisler, A. Jutla, L. Keefer, W. M. Brown, *Sci. Total Environ.* **2022**, *852*, 158448.
- [11] T. Prado, T. M. Fumian, C. F. Mannarino, P. C. Resende, F. C. Motta, A. L. F. Eppinghaus, V. H. Chagas Do Vale, R. M. S. Braz, J. D. S. R. De Andrade, A. G. Maranhão, M. P. Miagostovich, *Water Res.* **2021**, *191*, 116810.
- [12] P. Wityk, P. Sokołowski, M. Szczerska, K. Cierpiak, B. Krawczyk, M. J. Markuszewski, *J. Biophotonics* **2023**, *16*, e202300095.
- [13] M. Szczerska, P. Wityk, P. Listewnik, *J. Biophotonics* **2023**, *16*, e202200172.
- [14] R. Rashid, I. Shafiq, P. Akhter, M. J. Iqbal, M. Hussain, *Environ. Sci. Pollut. Res.* **2021**, *28*, 9050.
- [15] Y. C. Chuang, V. Tyagi, R. T. Liu, M. B. Chancellor, P. Tyagi, *Urol. Sci.* **2010**, *21*, 132.
- [16] M. Kruczkowski, A. Drabik-Kruczkowska, A. Marciniak, M. Tarczewska, M. Kosowska, M. Szczerska, *Sci. Rep.* **2022**, *12*, 1.
- [17] M. A. Moreno-Ibarra, Y. Villuendas-Rey, M. D. Lytras, C. Yáñez-Márquez, J. C. Salgado-Ramírez, *Mathematics* **2021**, *9*, 1817.
- [18] S. A. Hicks, I. Strümke, V. Thambawita, M. Hammou, M. A. Riegler, P. Halvorsen, S. Parasa, *Sci. Rep.* **2022**, *12*, 1.
- [19] L. Breiman, *Mach. Learn.* **2001**, *45*, 5.
- [20] A. Fisher, C. Rudin, F. Dominici, *J. Mach. Learn. Res.* **2018**, *20*, 1.
- [21] A. K. P. Anil, U. K. Singh, *J. Syst. Eng. Inf. Technol. (JOSEIT)* **2023**, *2*, 77.
- [22] T. Endo, H. Kajita, Y. Kawaguchi, T. Kosaka, T. Himi, *Biotechnol. J.* **2016**, *11*, 831.
- [23] W. B. Lee, Y. H. Chen, H. I. Lin, S. C. Shiesh, G. Lee, *Sens. Actuators B Chem.* **2011**, *157*, 710.
- [24] J. Jiang, H. Deng, H. Liao, X. Fang, X. Zhan, S. Wu, Y. Xue, *Front. Physiol.* **2022**, *13*, 864747.
- [25] A. Kowalczyk, J. P. Sęk, A. Kasprzak, M. Poplawska, I. P. Grudzinski, A. M. Nowicka, *Biosens. Bioelectron.* **2018**, *117*, 232.



- [26] N. Christodoulides, M. Tran, P. N. Floriano, M. Rodriguez, A. Goodey, M. Ali, D. Neikirk, J. T. McDevitt, *Anal. Chem.* **2002**, *74*, 3030.
- [27] W. L. Roberts, *Circulation* **2004**, *110*, e572. <https://doi.org/10.1161/01.CIR.0000148986.52696.07>
- [28] A. Aray, F. Chiavaioli, M. Arjmand, C. Trono, S. Tombelli, A. Giannetti, N. Cennamo, M. Soltanolkotabi, L. Zeni, F. Baldini, *J. Biophotonics* **2016**, *9*, 1077.

**How to cite this article:** P. Sokołowski, K. Cierpiak, M. Szczerska, M. Wróbel, A. Łuczkiwicz, S. Fudala-Książek, P. Wityk, *J. Biophotonics* **2024**, e202300523. <https://doi.org/10.1002/jbio.202300523>